International Journal of Innovative Technology and Exploring Engineering (IJITEE)
ISSN: 2278-3075 (Online), Volume-8 Issue-10, August 2019

Multiwall Carbon Nanotube Made Antenna At Terahertz Frequency Range

Niranjan Kumar, Saurabh Sambhav, Prakash Kumar, Srest Somay

Abstract: ***Earlier the propagation capability of BCNTs (bunch carbon nanotubes) made antenna was studied in terahertz frequency vicinity and its fulfilments were correlated with conventionally used thin gold film antenna. Those experiments were performed on the half-wave ribbon aerial of BCNTs and then on thin gold foil antennas which were resonated from 1THz to 50THz frequency range. To calculate its radiation efficiency they use both Moment of the moment (MOM) and potential integral equation (MPIE) technique. The numerical simulated result tells us that the radiation capability of a BNCTs of density 10^4 (CNTs/um) antenna has typically become smaller than the capability of gold foil antenna. We have experimented with replacing BCNT by MWCNT made antenna and studied its result on the same frequency range. After examination, we found that the interband transitions hinder big problems in MWCNT. It also hinders the propagation of guided wave and gives spoiling effect basically in the achievement of a fixed dimension MWCNT when we used it as an antenna.***

Index Terms: ***Multiwall Carbon Nanotube, Interband transitions, scattering parameters, gold carbon ribbon***

I. INTRODUCTION

1. OUTLINE

A multiwall CNT consists of N concentric shells, each shell is made of by wrapping of graphene layer and forms cylinder. The numeral shell in an MWCNT package in dimension from 3 to 201 with a distance between subsequent shells will be 03.39 to 03.59 A^0, which closed to distance of alternate layer in graphite by 03.35A^0. The lattice structure of the subsequent shells is commonly unrelated to one another with different chiralities [15], [26]. Further, the two subsequent shells of the MWCNT are said to be proportionate if the correspondence cell of unit length passes through with its CNT axis and is analytical to the demonstrate existence of translation similarity. [21], [22], [23], [24].

After numbers of experiments and analyze the electromagnetic properties of MWCNT, we face a lot of problems due to inter-shell interaction which leads to inner-shell electron tunneling. Due to that, we found different data in the same circumstances. By using selections rules for electrons and tunneling matrix and conservation law of energy and momentum. We conclude that the two incommensurable shells interact than in a different manner than two proportionate cells. That is the major advantage of MWCNT compare to SWCNTs.

A. Model

Our multiwall is a multi-shell structure of N coaxial, infinitesimal narrow cylinders in space. As each shell has a zigzag (m, 0) or an armchair (m, m) configuration, with m as an integer. Due to differences in the configuration of the thin cylinder shell our model can comprise both semiconducting and metallic shells [2], [5].

Let us consider the axis of MWCNT is along z-direction also the coordinate of the cylindrical system is (p, ϕ, z) and its centroid coincides with the origin of a co-ordinate cylindrical system.

Now we enumerate the shell of MWCNT, subsequent with 1 to N and will start with the inmost shell, due to their cross-sectional region that will be agreed with the position $R_N > R_{N-1} > \ldots . R_1$. As a cross-section region R_N, of an outer most shell, is imagined by us, is very much lesser than that of the wavelength of free-space. Thus for P^{th} shell P ϵ [1, N] possesses an axial conductivity per unit area and is denoted by σ_p [5]. Further, its transverse current density in each shell, along with inter-shell tunneling is neglected by us.

Let an electromagnetic field along related to azimuthal symmetry is very quickly excited in an MWCNT's with the homogeneous electric fields.

B. Figures

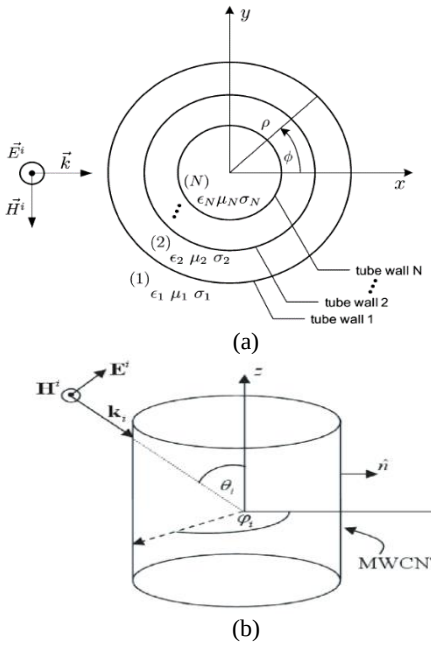

Fig. 1 (a) Equivalent model of MWCNT, (b) cylindrical coordinate view of model

Manuscript published on 30 August 2019.
*****Correspondence Author(s)
Niranjan Kumar, Physics Department, Amity University Patna/ Amity School of Engineering & Technology, Patna, India.
Saurabh Sambhav, Electronics Department, Amity University Patna/ Amity School of Engineering & Technology, Patna, India.
Prakash Kumar, Electical Department, Amity University Patna/ Amity School of Engineering & Technology, Patna, India.
Srest Somay, Metallurgy Department, NIT Waramgal, Andhra Pradesh, India.

II. MATH

Here electric Hertz vector $\Pi = \pi(\rho, z)e_z$ is governed by the Helmholtz equation

$$\frac{1}{\rho}\partial\frac{\partial}{x}\left(\rho\frac{\partial\pi}{\partial\rho}\right)+\frac{\partial^2}{\partial z^2}+k^2\Pi=0 \quad (1)$$

Where e_z = 'unity vector' along the z-axis.
Where, K = $\frac{w}{c}$ the wavenumber of free space.
C = speed of light in free space.
Since π depends only on z and ρ, then the component of electrical and magnetic fields are written as

$$E_\phi = 0, E_z = \pi\left(\frac{\partial^2}{\partial z^2}+k^2\right), E_\rho = \frac{\partial^2\Pi}{\partial\rho\partial z} \quad (2)$$

$$H_\phi = ik\frac{\partial\pi}{\partial z}, \quad H_z = 0, \quad H_\rho = 0 \quad (3)$$

Neglecting the inter shell tunneling, the two boundary conditions across the p[th] shell are [4].

$$-\frac{\partial\Pi}{\partial\rho}\Big|_{\rho=R_{p-0}}+\frac{\partial\Pi}{\partial\rho}\Big|_{\rho=R_{p+0}}=\frac{4\pi}{ikc}J_p \quad (4)$$

$$\pi\big|_{\rho=R_{p-0}}=\pi\big|_{\rho=R_{p+0}} \quad (5)$$

Here $J_p(z) = J_p(z)\, e_z$ is the current density of axial component on surface $\rho = R_p$, with

$$J_p(z)=\sigma_p\left(\frac{d^2}{dz^2}+k^2\right)\Pi(R_{p,z}) \quad (6)$$

Hence if σ_p is a surface conductivity on p[th] solitary shell's is available via quantum-transport calculations carried out in the tight-binding approximation as [4], [25].

$$\sigma_\rho(\omega)=-\frac{2\pi\omega ie^2}{hR_p\pi^2}\left\{\sum_{s=i}^{m}\int_{1stBZ}\frac{\partial F_c}{\partial p_z}\frac{\partial E_c}{\partial p_z}dp_z\times\frac{1}{\omega\left(\omega+\frac{i}{\tau}\right)}\right\}$$
$$-2\sum_{s=1}^{m}\int_{1stBZ}\varepsilon_c|R_{vc}|^2\times\frac{F_c-F_v}{h^2\omega\left(\omega+\frac{i}{\tau}\right)-4\in_c^2}dp_z \quad (7)$$

Where
e= charge on electron.
h = normalized planks constant.
p_z = axial projection of quasi momentum of an electron.
Index c = refers to the conduction band.
Index v = refers to the valance band. [6]
The first term of the above equation (7) corresponds to the intraband conductivity and the second term is the transition between the valence band and conduction band is known as interband transition. Further, the equilibrium Fermi Distribution functions are

$$F_c(P_z,S)=\left\{1+\exp\left[\frac{\in_c(P_z,S)}{k_BT}\right]\right\}^{-1} \quad (8)$$

and

$$F_v(P_z,S)=\left\{1+\exp\left[\frac{\in_v(P_z,S)}{k_BT}\right]\right\}^{-1} \quad (9)$$

The electron energies $\in_{C,V}(P_z,S)$ and normalized matrix element of the dipole transition R_{VC} for the Zigzag (m, 0) CNT are given by [1]

$$\in_c(P_Z,S)=-\in_V(P_Z,S)$$

$$=\gamma_0\sqrt{1+4\cos(ap_z)\cos\left(\frac{\pi s}{m}\right)+4\cos^2\left(\frac{\pi s}{m}\right)} \quad (10)$$

And

$$R_{VC}(P_z,S)=-\frac{b\gamma_0{}^2}{2\in_c^2}\times$$
$$\left[1+\cos(ap_z)\cos\left(\frac{\pi s}{m}\right)2\cos^2\left(\frac{\pi s}{m}\right)\right] \quad (11)$$

Where $\gamma_0 = 2.7_{eV}$ is the overlap integer [1]
And $a=\frac{3b}{2h}$,
$b = 0.142nm$ is the distance between two atoms in the graphene respectively.

By using Born approximation we can write the scattering power of an antenna is

$$P_r=\frac{\omega^2|\sigma_T|^2}{4c^3}\int_0^\pi\sin^3\theta\left|\int_{-L/2}^{L/2}e^{ikz\cos\theta}E_z^0(0,z)dz\right|^2d\theta \quad (12)$$

And its ohmic dissipation power lost is

$$P_t=\frac{1}{2}R_e(\sigma_T)\int_{-L/2}^{L/2}\left|E_z^0(0,z)\right|^2dz \quad (13)$$

Where, $\sigma_T=\sum_{p=1}^{N}(2\pi R_p\sigma_p)$ is per unit length and measure its ability to conduct electric current, equal to the reciprocal of the resistance of the substance an electrically narrow MWCNT.
Its efficiency is

$$\eta=\frac{P_r}{P_t}\sim\frac{|\sigma_T|^2}{R_e(\sigma_T)} \quad (14)$$

Where σ_T = Conductivity *per unit length.*

Retrieval Number: J95330881019/19©BEIESP
DOI: 10.35940/ijitee.J9533.0881019
Journal Website: www.ijitee.org

Published By:
Blue Eyes Intelligence Engineering and Sciences Publication (BEIESP)

III. RESULT AND DISCUSSION

In this experiment, we have noticed that the scattering property of confined size MWCNTs with radii R_N = 20 nm as well as R_N= 25nm at the Terahertz region. Here we first examine conductivity per unit length of a different length of electrical narrow MWCNTs by using equation (14).

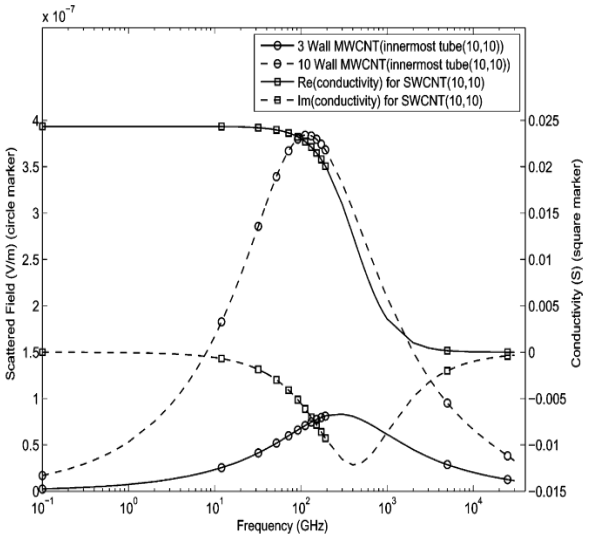

Fig. 2 (a) Graph Plotted between scattered field and frequency for a 3 and 10 wall MWCNT

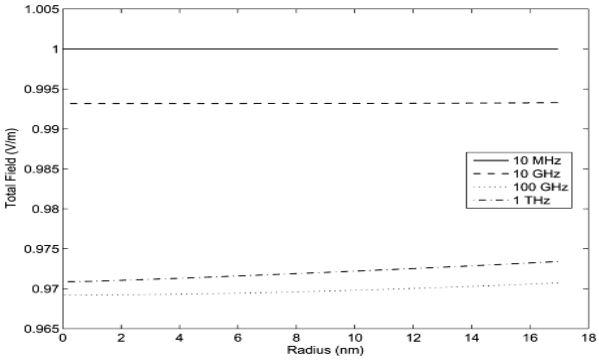

Fig. 2 (b) Graph plotted between Total Field (V/M) and radius (nm) of 50 wall MWCNT.

From the above fig. 2 (a) we plot a graph between (N = 1) SWCNTs along with [N ∈ (2, 4)] MWCNTs, (where σ_T have the strongest resonance). From the graph, we see that the resonance becomes weaker when N goes up and we found it almost disappears when N>10. Now we are explaining the above facts in the following way. As we increase the terahertz frequency from 1Hz to 50Hz the surface conductivity σ_p of the P[th] shell obtained from equation (7) has much more resonance compare to the van home singularity. If the resonance of different shell overlaps, then it is necessary to consider the weighted summations of the surface conductivity of all shells. From equation (14) we can say that σ_T does not evince resonance behavior in the infrared region.

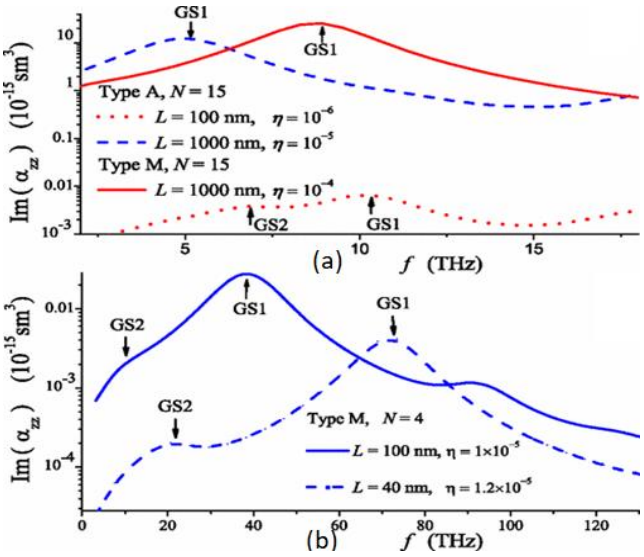

Fig. 3 (a,b) Graph plotted between Im (αzz) and frequency (THz).

Let us consider an isolated shell of radius R_N ~ R_N>5nm whose conductivity is per unit length, also have a closely spaced large number of resonance, for this reason, bands appear in the spectrum, instead of discrete lines. Further for R_N = 10.22 mm i.e. N = 29 shells its imaginary and real parts of dynamic conductivity σ_T per unit length are presented in fig. 4.

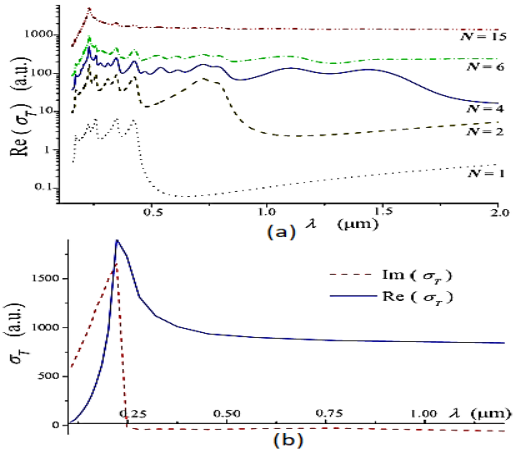

Fig. 4 (a) Graph plotted between Real and (b) Imaginary part of σT verses wavelength λ

From fig.4 (a) it is clear that σ_T (the real part) increases with the increases in frequency and has a maximum value near f = 1304 THz (i.e. $\lambda = 230nm$, it is a Plasmon resonance frequency not a geometric resonance frequency. Further after calculation by using equation (13) we observed that the power of scattering (P_t) for that MWCNT is same as $|\sigma_T(\omega)|^2$. We also observed that the efficiency of MWCNT antenna increases with shells and it moves towards unity as shell becomes narrow MWCNTs. For frequency of 600THz the calculation made by us is n = 0.44 for N = 140 and also n = 0.17 for N = 70.

Retrieval Number: J95330881019/19©BEIESP
DOI: 10.35940/ijitee.J9533.0881019
Journal Website: www.ijitee.org

Published By:
Blue Eyes Intelligence Engineering and Sciences Publication (BEIESP)

IV. CONCLUSION

The efficiency of MWCNTs antenna will be increased with the increase in the numbers of shell N. We also found that the value at which the efficiency of the antenna depends only upon its natural characteristics of MWCNT. For unit efficiency we have to suppress strongly the impact of quantum size effect by using the highest cross-sectional area of MWCNTs. But in the gold nanowire, the quantum size effect does not pronounce up to a cross-sectional area of a few tens of nanometers. Thus we can say emphatically that the MWCNTs have sufficient high efficiency up to n~0.1and can operate in a wide range of frequency up to the visible region. Further we noticed that the interband transitions hinder big problems in MWCNTs antenna because the propagation of guided waves is hindered by the interband transitions and gave an injurious response in the conduction of the propagation of waves when it is used as an antenna.

REFERENCES

1. M. V. Shuba. “Theory of multiwall carbon nanotubes as waveguides and antennas in the infrared and the visible regimes”, Physical review B, 04/2009.
2. M. V. Shuba. “Electromagnetic wave propagation in an almost circular bundle of closely packed metallic carbon nanotubes” Physical Appraisal B, 10/2007.
3. M.S. Dresselhaus, G. Dresselhaus, and Ph. Avouris, Carbon Nanotubes (Springer, Berlin, Germany, 2001).
4. S. Reich, C. Thomsen, and J. Maultzsch “Carbon Nanotube, Basic Concepts and Physical Properties” (Wiley-VCH, Berlin, Germany, 2004).
5. M. L. Schipper, N. Nakayama – Rachhford, C. R. Davis, N. W. S. Kam, P. Chu, Z. Liu, X. Sun, H. Dai, and S. S. Gambhir, “ Nature Nanotechnology “. 3, 216 (2008).
6. G. Ya. Slepian, S. A. Maksimenko, A. Lakhtakia, O. Yevtushenko, and A. V. Gusakov, Phys. Rev. B 60, 17136 (1999).
7. S. A. Maksimenko and G.Ya. Slepian, “In Electromagnetic Fields in Unconventional Materials and Structures” (O. N. Singh and A. Lakhtakia, Eds.) (Wilei, New Yourk, NY, USA, 2000), pp 217-255.
8. S. A. Maksimenko and G. Ya. Slepian, “Nano electromagnetics of low-dimensional structures, in Nanometer Structures: Theory, Modeling and Simulation” (A. Lakhtakia, ed) (SPIE Press, Bellingham. WA, USA. 2004), pp, 145-206.
9. M. J. Hagmann, IEEE Trans. “Nanotechnology” 4, 289 (2005).
10. J. Rybcznski. K. Kempa, A. Herczynski, Y. Wang, M. J. Naughton. Z. F. Ren, Z. P. Huang, D. Cai, and M. Giersig, Appl. Phys. Lett. 90 021104 (2007).
11. A. Raychowdhury and K. Roy, IEEE Trans, CAD Integrated, Circ. Syst. 25, 58 (2006).
12. A. G. Chiariello and G. Miano, COMPEL Int. J. Comp. Math. Electrical Electron. Engg, 26 571 (2007).
13. A. Maffucci, G. Miano, and F. Villone, Int. J. Circ. Theory Appl. 36. 31 (2008).
14. H. Li, W. Y. Yin, K. Banerjee, and J. F. Mano, IEEE Trans Electron Device.
15. Y. Wang, K. Kempa, B. Kimball, J. B. Carlson, G. Benham, W. Z. Li, T. Kimball, J. Rybczynski, and Z. F. Ren, Appl. Phys. Lett. 85, 2607 (2004).
16. G. W. Hanson, IEEE Antennas Propagat. Mag. In press, June (2008).
17. M. Ge and K. Sattler, Science 260, 515 (1991).
18. J. Hao and G. W. Hanson, Phys. Rev. B 74, 035119 (2006).
19. J. Hao and G. W. Hanson, Phys. Rev. B 75, 165416 (2007).
20. O. V. Kibis and M. E. Portnoi, Tech. Phys. Lett. 31, 671 (2005).
21. O. V. Kibis, M. Rosenan de Costa, and M. E. Portnoi, Nano Lett. 7, 3414 (2007).
22. S. Bandow, M. Takizawa, K. Hirahara, M. Yudasaka, and S. lijima, Chem. Phys. Lett. 337, 56 (2001).
23. S. Wang and M. Grifoni, Phys. Rev. Lett. 95, 266802 (2005).
24. R. Saito, G. Dresselhaus, and M. S. Dresselhaus, Appl. Phys. 73, 494 (1993).
25. P. Lambin, V. Meunier, and A. Rubio, Phys. Rev. B 62, 5129 (2000).
26. K. H. Ahn, Y. H. Kim, J. Wiersig and K. J. Chang, Phys. Rev Lett 90. 026601 (2003).
27. S. A. Maksimenko, A. A. Khrushchinsky, G. Ya. Slepian, and O. V. Kibis, J. Nanophoton,1, 013505 (2007).
28. S. Iijima, Nature (London) 354, 56 (1991).

AUTHORS PROFILE

Niranjan Kumar, Physics Department, Amity University Patna/ Amity School of Engineering & Technology, Patna, India.

Saurabh Sambhav, Electronics Department, Amity University Patna/ Amity School of Engineering & Technology, Patna, India.

Prakash Kumar, Electical Department, Amity University Patna/ Amity School of Engineering & Technology, Patna, India.

Srest Somay, Metallurgy Department, NIT Waramgal, Andhra Pradesh, India.